DOI: 10.1002/cbic.200800732

Electrochemical and Conformational Consequences of Copper (Cu^{I} and Cu^{II}) Binding to β-Amyloid(1–40)

Maria Brzyska[†],[c] Katarzyna Trzesniewska,[c] Agnieszka Wieckowska,[b] Andrzej Szczepankiewicz,[c] and Danek Elbaum*[a]

Extracellular deposits of β-amyloid (Aβ) into senile plaques are the major features observed in brains of Alzheimer's disease (AD) patients. A high concentration of copper has been associated with insoluble amyloid plaques. It is known that Aβ(1–40) can bind copper with high affinity, but electrochemical properties of Aβ(1–40)–Cu complexes are not well-characterised. In this study we demonstrate that complexation of copper (both as Cu^{I} and Cu^{II}) by Aβ(1–40) reduces the metal electrochemical activity. Formation of copper-Aβ(1–40) complexes is associated with alteration of the redox potential. The data reveal significant redox activity of fresh Aβ–copper solutions. However, copper-induced structural rearrangements of the peptide, documented by CD, correspond with time-dependent changes of formal reduction potentials ($E^{0'}$) of the complex. Fluorescent and electrochemical (cyclic voltammetry and differential pulse voltammetry) techniques suggest that reduction of the redox activity by Aβ–Cu complexes could be attributed to conformational changes that diminished copper accessibility to the external environment. According to our evidence, conformational rearrangements, induced by copper binding to amyloid, elongate the time necessary to attain the same β-sheet content as for the metal-free peptide. Although the redox activity of Aβ–Cu complexes diminishes in a time-dependent manner, they are not completely devoid of toxicity as they destabilize red blood cells osmotic fragility, even after prolonged incubation.

Introduction

Alzheimer's disease (AD) is one of the most common progressive neurodegenerative disorders. Although senile plaques are considered as the main pathological hallmarks of AD, a better correlation between cognitive impairment and concentration of the Aβ soluble forms has been reported.[1] A direct toxic effects of Aβ to human and rat hippocampal cell cultures were reported several years ago[2] and suggest that Aβ is an essential plaque constituent that participates in the pathogenesis of AD.

Oxidative stress has been implicated as a potential mechanism participating in the neurotoxicity of Aβ-mediated interactions responsible for AD etiology.[3,4] Aβ-mediated radical formation was postulated by Hensley and co-authors.[5] Radical generation was manifested by formation of lipid and protein oxidation products[6,7] and increased concentration of cellular H_2O_2.[8]

Elevated levels of several metals (copper, zinc and iron) inside neuropil of the cortical basal nuclei of the amygdala were reported for the AD patients.[9] In addition, direct binding of redox active metals like copper and iron, was reported to enhance Aβ neurotoxicity.[10] Aβ is capable of generating redox active species even in cell free solutions.[11] In a cell free system it was demonstrated that Aβ can bind copper thus leading to redox activity and oxidative modifications of the peptide.[12,13]

Copper coordination to Aβ through His6, His13 and His14 yields binding with a high affinity ($1.6\times10^{17}\,M^{-1}$ for Aβ42).[14,15] Although a model assuming four-ligand-coordinating Cu^{II} in a planar configuration has been proposed for Aβ–Cu^{II} complexes,[16] the fourth ligand is still unclear. The candidate residues include Tyr10,[17] N-terminal nitrogen[18] or an unspecified carboxylate side chain.[19] However, a second copper binding site, characterised by constant K_d of approximately 1.6 μM has also been suggested.[20,21] Tyr10 and Met35 residues were suggested to participate in the redox activity of Aβ,[22,23] but their roles are still disputable.[24] It was reported that Aβ is able to reduce Cu^{II} to Cu^{I}.[25] However, recent findings questioned this observation.[24] On the other hand, antioxidant properties of Aβ were also postulated.[26]

Copper uptake by human brain is mediated largely by copper transport (CTR) proteins (mainly hCTR1—the human copper transporter) as Cu^{I},[27] and, to lesser extent, as Cu^{II}, by DMT1, the relatively nonspecific divalent cation transporter.[28] Following the uptake from blood by the cell transporters, metal delivery by a series of protein-specific chaperones, such

[a] *Prof. D. Elbaum*
Institute of Physics, Polish Academy of Sciences
al. Lotnikow 32/46, 02-668 Warsaw (Poland)
Fax: (+48) 22-843-09-26
E-mail: elbaum@ifpan.edu.pl

[b] *Dr. A. Wieckowska*
Department of Chemistry, Warsaw University
Pasteura Street 1, 02-093 Warsaw (Poland)

[c] *Dr. M. Brzyska, Dr. K. Trzesniewska, A. Szczepankiewicz*
Department of Neurophysiology
Nencki Institute of Experimental Biology, Polish Academy of Sciences
Pasteura Street 3, 02-093 Warsaw (Poland)

[†] *Deceased*

Supporting information for this article is available on the WWW under http://dx.doi.org/10.1002/cbic.200800732.

as Atox1 or CCS to the apoenzymes takes place. Thus, disruption of the metal homeostasis in such a delicate system may cause a temporary release of copper. Hence, copper binding by intracellular or vascular Aβ may lead to the formation of both Aβ–Cu^{II} and Aβ–Cu^{I} complexes. Additionally, bathocuproine chelating studies of AD senile plaques support the possibility that Aβ–Cu^{I} aggregates occur in the brain.[29] However, according to our knowledge, neither experimental data concerning binding of Cu^{I} by Aβ nor the properties of Aβ–Cu^{I} complexes have been convincingly presented yet.

In order to understand the role of copper in Aβ electrochemical reactivity we investigated the influence of metal binding (Cu^{I} as well as Cu^{II}) on the protein secondary structure, hydrophobicity, redox potentials and formation of oxidation product from redox-sensitive fluorescent probe (H_2DCF). We compared redox properties of free copper ions in solution and the ones complexed by Aβ. The influence of time-induced changes of copper-Aβ complexes was correlated with their redox properties. To mimic early stages of Aβ formation, both the peptide and its copper complexes were kept soluble during the measurements. In addition, copper and copper-amyloid complex ability to induced red blood cell lysis was used as a model for the damaging effects of the peptide towards the cell membrane.

Results

In order to establish the nature of copper (Cu^{I} and Cu^{II}) interaction with Aβ we have applied several independent methods. Formation of metal-Aβ complexes was documented by a copper-sensitive fluorescence probe (Phen Green™). The ion's ability to alter Aβ conformation was followed by two independent methods: using CD and a structure sensitive fluorescent probe (bisANS). In addition, we employed voltammetry (CV and DPV) and redox susceptible fluorescence probe (H_2DCF) to determine Aβ's ability to change redox properties of copper. Finally, we used human erythrocytes to test if oxidative properties of Cu^{II}, as determined by its ability to induce direct red cell lysis, are altered in the presence of the Aβ–Cu^{II} complex.

Figure 1 summarizes the effects of Cu^{I} and Cu^{II} on a metal binding indicator Phen Green™. This phenanthroline based fluorescent probe is a sensitive metal sensor able to detect binding of low copper concentrations as registered by a strong fluorescence quenching.[30] According to the producer, PG complexes with Cu^{I} and Cu^{II} have slightly different spectral properties, generating differences of the dye quenching by the same concentrations of the metal. As shown in Figure 1, copper forms complexes with Aβ easily detectable at 100 nM copper and 100 nM Aβ concentration. The peptides' ability to decrease copper induced Phen Green™ fluorescence quenching results from its capability to interact with Cu^{I} and Cu^{II}, thus preventing the probe binding. However, further increase of PG fluorescence by Aβ incubated for 2 h with copper, in comparison to that caused by fresh complexes, suggests that the time-induced interactions within the complex make the metal more tightly bound to the peptide and/or less accessible to the solution. Note that the Aβ alone has an insignificant effect on the PG quenching.

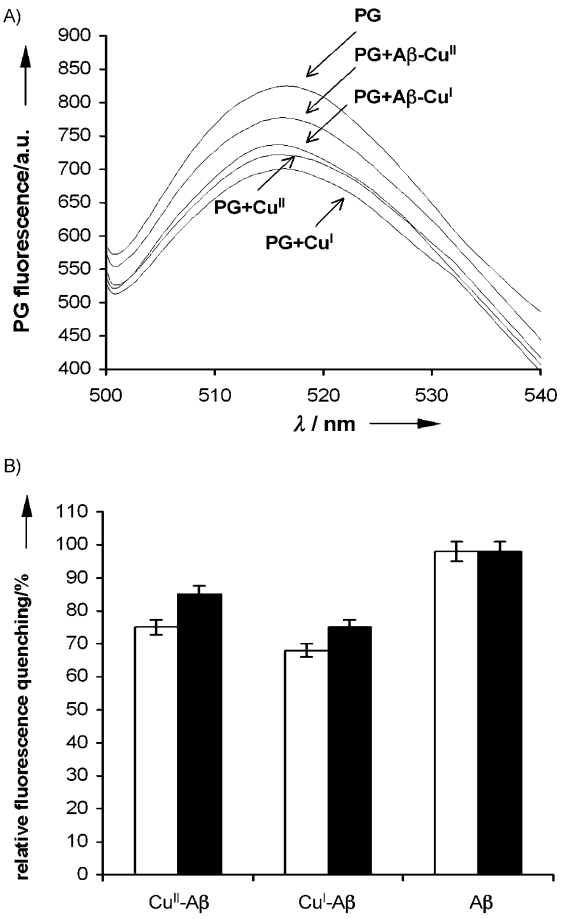

Figure 1. A) Effect of Aβ, Cu^{I}, Cu^{II} and Aβ–copper complexes on the fluorescence (emission) spectra of PG. B) PG relative fluorescence changes in the presence of complexes of Aβ–Cu (freshly prepared (open bars) or incubated for 2 h-(closed bars)). PG relative fluorescence quenching was defined as described in Experimental Section. All samples were in 5 mM MOPS, pH 7.2, PG concentration was 200 nM, Aβ was 100 nM and Cu (both Cu^{II} and Cu^{I}) 100 nM.

The ability of copper to alter Aβ conformation was confirmed by a probe sensitive to available nonpolar cavities in proteins. BisANS binding to hydrophobic domains present in proteins, including Aβ,[31] results in a fluorescence increase and a blue shift of the dye fluorescence peak. The residues 13–21 and 30–36 were suggested as potential bisANS binding regions of Aβ structure.[32] His13 and His14, the two residues coordinating copper, are localized in the first peptide region binding bisANS; this makes the probe potentially responsive to hydrophobicity changes induced by the metal binding. While binding of the probe to the peptide generated quite a large fluorescence increase, binding to Aβ–Cu^{II} complex resulted in an even higher fluorescence (Figure 2). In contrast, interaction of the dye with Aβ–Cu^{I} yielded slightly lower fluorescence. Different fluorescence of bisANS bound to the Aβ–copper complexes could be a result of dissimilar accessibility of the peptide hydrophobic domains in comparison with those of the copper-free Aβ, probably due to different conforma-

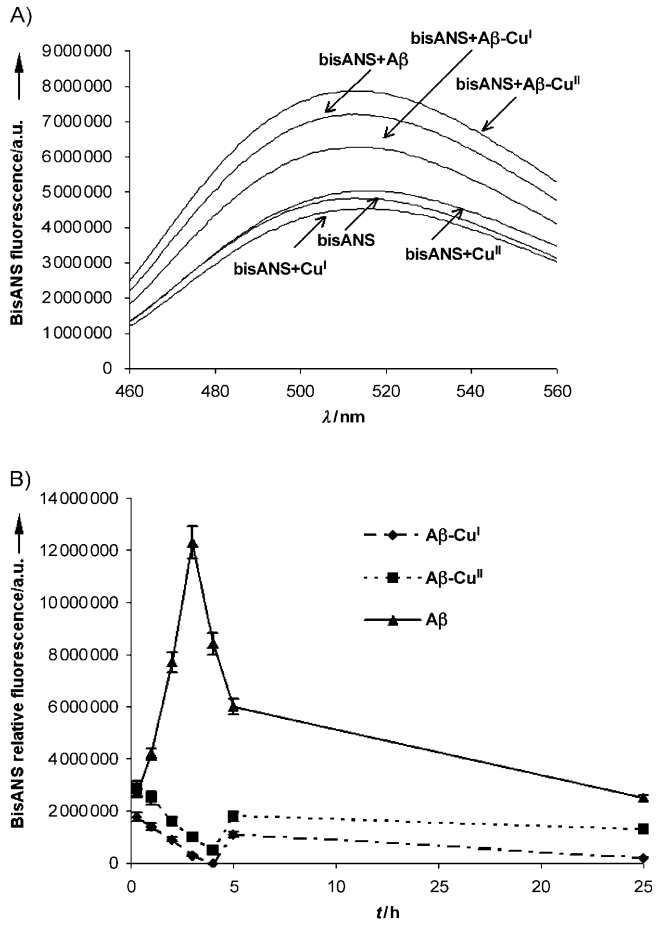

Figure 2. A) Effect of 400 nM Aβ, 2 μM Cu^{II} or Cu^{I} on 0.2 mM bisANS fluorescence spectra in PBS pH 7.2, measured immediately after Aβ–Cu complex formation. B) Changes of bisANS relative fluorescence (corrected for fluorescence in the absence of Aβ) induced by the time-dependent structural rearrangement of Aβ–Cu complexes.

tions. However, a fast decrease of bisANS binding, as judged from the diminished fluorescence signal observed after incubation of the complex, suggest time-dependent folding of Aβ complexes that decreased the exposure of hydrophobic domains to bisANS (Figure 2). Time dependent changes of metal-free β-amyloid showed an increase of bisANS fluorescence up to 3 h. After that time a gradual decrease was observed, similarly to reported by Kremer and coauthors,[33] consistent with the onset of the aggregation process.

To characterise Aβ–copper complexes, their CD spectra were examined. A range of 190–250 nm (far UV) represents amide chromophore region informing about secondary structure of the peptide, while longer wavelengths (250–400 nm; near UV) bear information about aromatic side chains (250–300 nm) or extrinsic chromophores (including metal ions) transitions. Although contribution of near-UV transitions may affect far-UV spectra thus complicating secondary structure analysis, amide chromophore dominates in the far UV, approximately by the factor of 10.[34] To confirm the effect of copper on the components of Aβ secondary structure we analysed CD spectra in the 190–250 nm range (Figure 3). Under the experimental conditions, the predominant Aβ secondary structure is that of β-

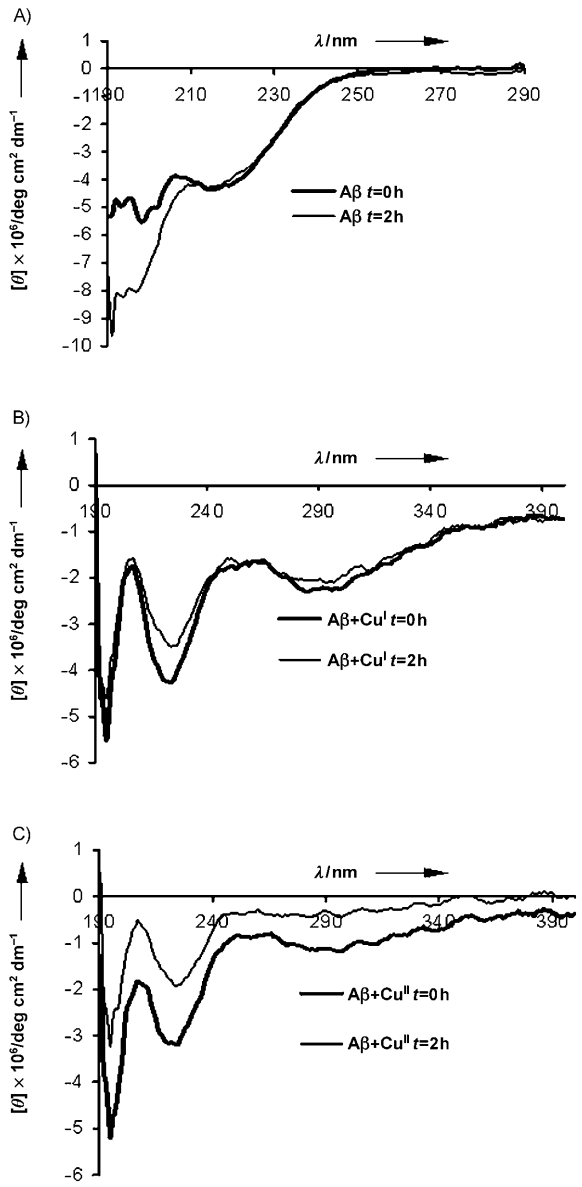

Figure 3. Effect of Cu^{I} and Cu^{II} on the CD spectra of Aβ.

sheet (47%), 2 h incubation enhances its content to 55% (Table 1), most likely due to time dependent protein folding that precedes aggregation. Addition of stoichiometric quantities of copper (both Cu^{I} and Cu^{II}) lowered the β-sheet content and increased the random coil conformation. Interaction of Aβ with Cu^{I} or Cu^{II} resulted in an appearance of a new peak near

Table 1. Effect of Cu^{II} on the components of Aβ secondary structure as determined by CD spectroscopy analyzed by using CD Neural Network (CDNN).

structure	Aβ		Aβ–Cu^{II}		Aβ–Cu^{I}	
	$t=0$	$t=2$ h	$t=0$	$t=2$ h	$t=0$	$t=2$ h
helix	16%	12%	12%	13%	15%	13%
β-sheet	47%	55%	42%	44%	40%	42%
β-turn	17%	16%	15%	16%	16%	16%
random coil	20%	17%	31%	27%	30%	29%

205 nm (Figure 3). The height of this peak was proportional to the increasing ratio of copper to Aβ (data not shown). The 250–400 nm range of CD spectra of Aβ–Cu^{I} showed the metal to ligand charge transfer band characteristic for a d^{10} configuration around 300 nm. In this region the CD spectra were more negative than those of Aβ–Cu^{II} that are characterised by a d^{9} configuration and the ligand to metal charge transfer band, suggesting possibility for a different geometry of the complexes. Time-dependent changes, (in the case of Cu^{I} only in the regions of 195 nm and 220 nm, in the case of Cu^{II} also in the region of 205 nm) may be consistent with this hypothesis. Generally, incubation of the Cu-Aβ complexes for 2 h resulted in an increase of the β-sheet structure with a concomitant random coil decrease, thus leading to a conformation resembling the Aβ conformation without the metal (Table 1). However, the conformational changes were much slower than those of metal-free peptide.

Electrochemical consequences of copper ability to interact with Aβ were observed based on voltammetric measurements, and the results are presented in Figures 4 and 5 and Figure S4 in the Supporting Information. Voltammetry is a convenient method to monitor subtle changes in redox properties of the electroactive species reflecting their interactions. In the present paper we employ cyclic and differential pulse voltammetry to follow the changes of the Cu^{II}-related electrode processes in the absence and presence of Aβ. Cyclic voltammetry (CV) is a technique that is most widely used to get the information about electrochemical reactions. CV consists of linearly scanning potential applied to the solid electrode using triangular waveform of potential. Differential pulse (DPV) is a pulse voltammetric technique and is based on sampled current potential-step experiments. A sequence of such potential steps is applied to the working electrode. In differential pulse voltammetry potential pulses are superimposed on linear changing potential. The current is sampled twice—just before the pulse application and at the end of duration of each pulse. More information about the methods may be found elsewhere.[35]

Copper ions in KCl solution were reduced in two steps [Eqs. (1) and (2)]:

$$Cu^{II} + e = Cu^{I} \quad (1)$$

$$Cu^{I} + e = Cu^{0} \quad (2)$$

observed as peaks c1 and c2.

Accordingly, oxidation processes observed after reversal of the potential are as follows [Eqs. (3) and (4)]:

$$Cu^{0} - e = Cu^{I} \quad (3)$$

$$Cu^{I} - e = Cu^{II} \quad (4)$$

As shown in Figure 4A, C and E, the formal potentials of the reduction processes are $E_1^{0\prime} = 0.17$ V, and $E_2^{0\prime} = -0.26$ V respectively, similarly to observed by Słowinski .[36] The CV data reveal that in the presence of Aβ the first step of Cu^{II} reduction is shifted towards more negative potentials (about 60 mV; Figure 4B, D and F). It means that reduction of Cu^{II} bound to Aβ is more difficult that the reduction of unbound Cu^{II} ions. The process is concentration-dependent and in the case of 200 mM Cu^{II} value of the shift increases to 100 mV. Oxidation of Cu^{I} to Cu^{II} (Eq. 4) in the presence of the peptide is shifted towards more positive potentials (to 0.25 V approximately). Lowering of the peak current in the presence of Aβ was observed during reduction as well as during oxidation process (Figure 4), suggesting lower value of diffusion coefficient of Aβ–Cu^{II} complex compared to the complex of Cu^{II} with chloride ions. As confirmed by DPV, lower current peak is also a result of the lower electrochemically active concentration of copper, possibly due to copper complexation by Aβ (Figure 4E and F). Moreover, separation of the reduction from oxidation potential peaks resulting from lower reduction potential and higher oxidation potential in the presence of Aβ, suggests chemical irreversibility and can be understood in terms of chemical reaction between Cu^{II} and Aβ. As seen in the voltammetric curves recorded in a longer potential range (Figure 4C and D). In the presence of Aβ the reduction peak potential of (2) is even more shifted towards more negative values. It may suggest that reduction of Cu^{I} in the presence of the peptide is more difficult than reduction of Cu^{II}. Thus it is conceivable that Aβ–Cu^{I} complexes may be more stable than Aβ–Cu^{II} ones. Beer and coauthors[37] proposed an approach that links stability constants of a complex in different oxidation states with measurable redox potentials; this allows for the calculation of binding enhancement factor (BEF). BEF equal to K_{ox}/K_{red} may be calculated from Equation (5):

$$\Delta E_f(nF/RT) = \ln(K_{ox}/K_{red}) \quad (5)$$

where ΔE_f is the difference between formal potentials of copper in presence and absence of Aβ. K_{red} and K_{ox} are the stability constants of complexes with Aβ in different oxidation states of copper. The rest of the symbols has their standard meaning.

The BEF value for reaction (1) is 10.34. This is in agreement with other observations that Cu^{II} ions form complex(es) with Aβ. The BEF factor for the second step of reduction process is even higher (2413.12) than the factor calculated for the Cu^{II} with Aβ. This means that Cu^{I} binds to Aβ stronger than Cu^{II}.

Additionally, data registered in a longer potential range (Figure 4C and D) reveal appearance of the third peak of reduction (−1.15 V) that is not visible in solutions containing copper only, but observed in the presence of Aβ. It can be assumed that the third peak may represent one-step reduction of an undefined Aβ–Cu complex to the Cu^{0}. Possibility of the reduction to Cu^{0} comes from the observation that the anodic potential demonstrates only two peaks of Cu oxidation, that of reaction (3) being significantly higher in the presence of Aβ than in copper only solutions; this suggests that it represents oxidation of a sum of species reduced to Cu^{0}.

Figure 5 depicts a significant effect of the Aβ–Cu^{II} complex incubation time (0–16 h) on the observed CV and DPV curves. The CV signal reveals a time-dependent separation between oxidation and reduction potentials and decrease of the peak

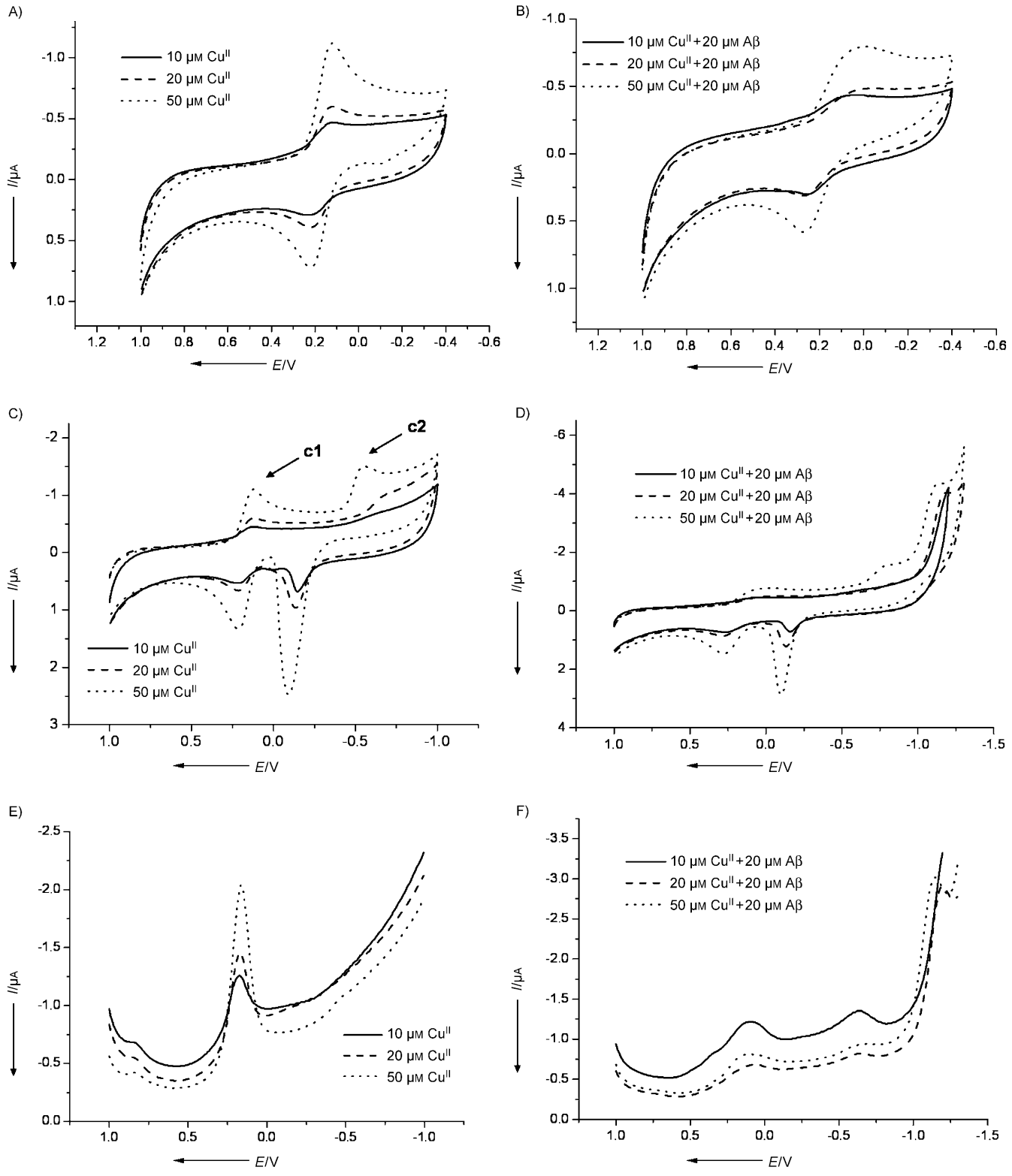

Figure 4. A comparison of cyclic (panels A–D) and differential pulse (E, F) voltammograms of free copper (A, C, E) and Aβ–copper complexes (B, D, F) in 0.2 M KCl under oxygen free conditions. Copper concentration range: 10–50×10^{-6} M, Aβ concentration: 20×10^{-6} M.

currents, consistent with changes in Aβ–Cu^{II} complex structure and electrochemical properties (Figure 5 A). A DPV curve confirms the decrease of all peaks registered during incubation; this suggests formation of more stable Aβ–Cu complexes (Figure 5 B). Moreover, the plot shows two peaks of Cu^{II} to Cu^{I} reduction, one at the 0.15 mV and second at 0 mV. Faster decrease of the first peak suggests that it represents more labile species. Based on our electrochemical results, we assume that

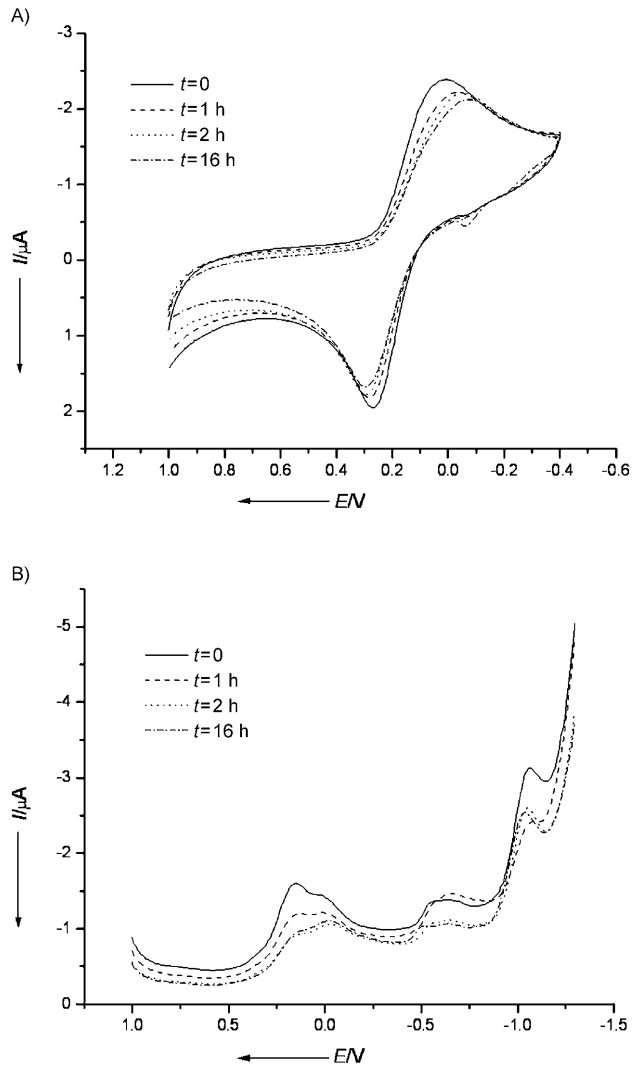

Figure 5. Time-dependent changes of electrochemical properties of Aβ–copper complexes (1:10), as demonstrated by cyclic (A) and differential pulse (B) voltammetry. Voltammograms were registered immediately ($t=0$) after Aβ to copper addition, and after 1, 2 or 16 h incubation of the complex.

time-dependent folding of Aβ–Cu complex may cause the observed changes.

In the presence of PBS, representing a more "physiological" approach towards buffering system, the formal potentials of copper reduction processes are $E_1^{0\prime}=-0.02$ V, and $E_2^{0\prime}=-0.75$ V respectively, while in the presence of Aβ the first step of Cu^{II} reduction is less shifted towards more negative potentials (about 30 mV) and the second one disappears (Figure S1). We observed these effects under stoichiometric ratios of Cu^{II} to Aβ (2:1, or less). This may suggest that Cu^{II} complexes with Aβ are soluble in PBS during all time of the experiment. The other observation is that Aβ does not block the electrode surface, as judged by the fact that addition of Aβ did not change the voltammograms and no decrease of background is seen and the height of c1 peak remains unchanged. Reproducible disappearance of the c2 peak upon addition of Aβ and its reappearance when the excess of Cu^{II} was added is consistent with the peptide interaction with Cu^{I} form as well. Data registered after 2 h of incubation of Aβ–Cu demonstrate a decrease of the peak current, that can be attributed to the complex folding. Generally, conclusions drawn from both analytical systems are comparable. However, presence of relatively high concentrations of the Cu-binding phosphates creates less favourable conditions for electrochemical measurements in PBS.

Independent evidence that Aβ is capable to modulate copper redox activity was collected applying a redox sensitive fluorescence dye H_2DCF, used both in cells and cell-free systems. The probe was also used to detect oxidative properties of metals.[38] Although the chemistry of the dye oxidation is complicated and has not been fully characterised yet, it is known that last stage of multiple intermediate steps leading to final oxidation to DCF requires participation of H_2O_2 or O_2.[39] As the electrochemistry data did not suggest production of H_2O_2 by Aβ–Cu complexes, to meet this requirement, PBS used in these experiments was not deaerated. Figure 6 summarizes the effect of Cu^{I}, Cu^{II} and Aβ–copper complexes on the H_2DCF oxidation as measured by fluorescence increase of the probe oxidized form. Due to the fact that the H_2DCF is nonfluorescent and the probe fluoresces upon oxidation to DCF, the appearance of the signal reports only the redox ability of copper and copper-Aβ complexes. While the ability of Cu^{II} alone to

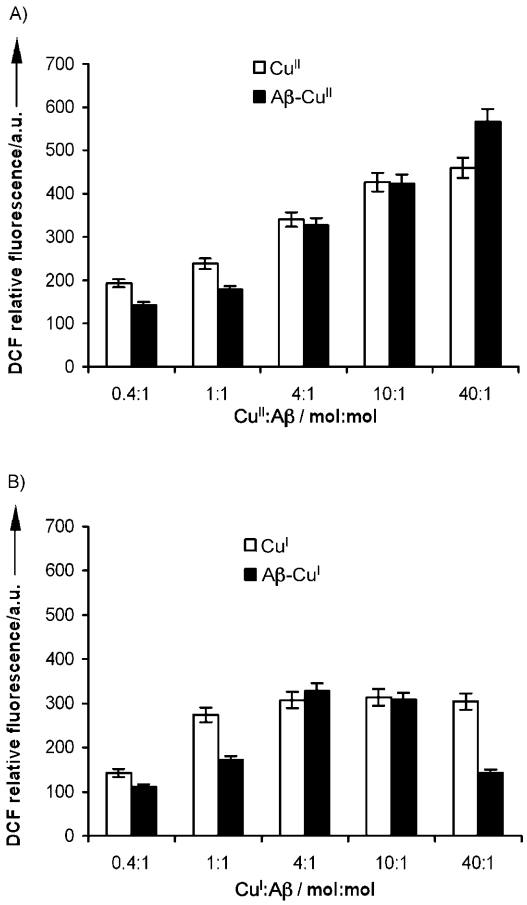

Figure 6. Influence of A) Cu^{II} and B) Cu^{I} concentration on DCF generation in the presence of Aβ (500 nM). Experiment carried out in air oxygen equilibrated PBS.

oxidize H_2DCF is concentration dependent in a defined range of dye and metal concentrations (data not shown), the ability of the Aβ–Cu^{II} complex to oxidize H_2DCF is dependent on the ratio of Cu^{II} to the peptide (Figure 6A). Note that for the complex formed at substoichiometric ratios of Cu^{II} to Aβ the reactivity towards H_2DCF is lower than that of Cu^{II} alone. On the other hand, at higher ratio of Cu^{II} to Aβ the complex was more reactive than the ion alone (Figure 6A). Although much lower, oxidation of the dye in the presence of Cu^{I} ions was also observable. We attribute this unexpected effect to the possibility of Cu^{I} oxidation by the dissolved oxygen and/or by-products of H_2DCF oxidation. Interestingly, oxidation of H_2DCF by Cu^{I} complexes with bathocuproine were also described.[40] Slight DCF generation in the presence of Aβ–Cu^{I} complexes was observed only at the 4-10 :1 ratios of metal to peptide (Figure 6B). Oxidation of Cu^{I} to Cu^{II} by the dissolved oxygen did not exceeded 10% of the monovalent metal per hour, as measured by a bathocuproine fluorescence quenching assay.[41] It was also demonstrated that the Aβ–Cu^{I} complex catalyzed the reduction of oxygen to produce hydrogen peroxide,[24] which could then oxidize H_2DCF.

In order to assess the potential biological relevance of copper binding to β-amyloid we examined the complex's propensity to interact with erythrocyte membranes (Figure 7A). Copper-induced spontaneous lysis of erythrocyte membranes is a well-known phenomenon,[42] however it occurs at micromolar concentrations of the metal and above (Figure 7A). To approach the assay towards more physiological concentration of Aβ, we diminished Cu^{II} concentration to 100 nM and simultaneously applied moderate hypotonic stress (0.42% NaCl). The effect of Cu^{II} concentration on the relative haemolysis is presented in Figure 7A (insert). In the presence of Aβ–Cu^{II} complex we observed lower haemolysis of red blood cells (RBCs) compared to Aβ and Cu^{II} alone (Figure 7B). This effect was time dependent (Figure 7B insert). In contrast, similar concentrations of aggregated, fibrillar Aβ together with hypotonic stress induced higher RBC haemolysis (58%). Similar results were observed for Aβ aggregated in the presence of Cu^{II} (57%), although morphology of aggregates differed significantly (Figure S3). We attribute this result to a high affinity of aggregated Aβ to RBCs, characterised by a more efficient binding of larger aggregates to red cells.[43]

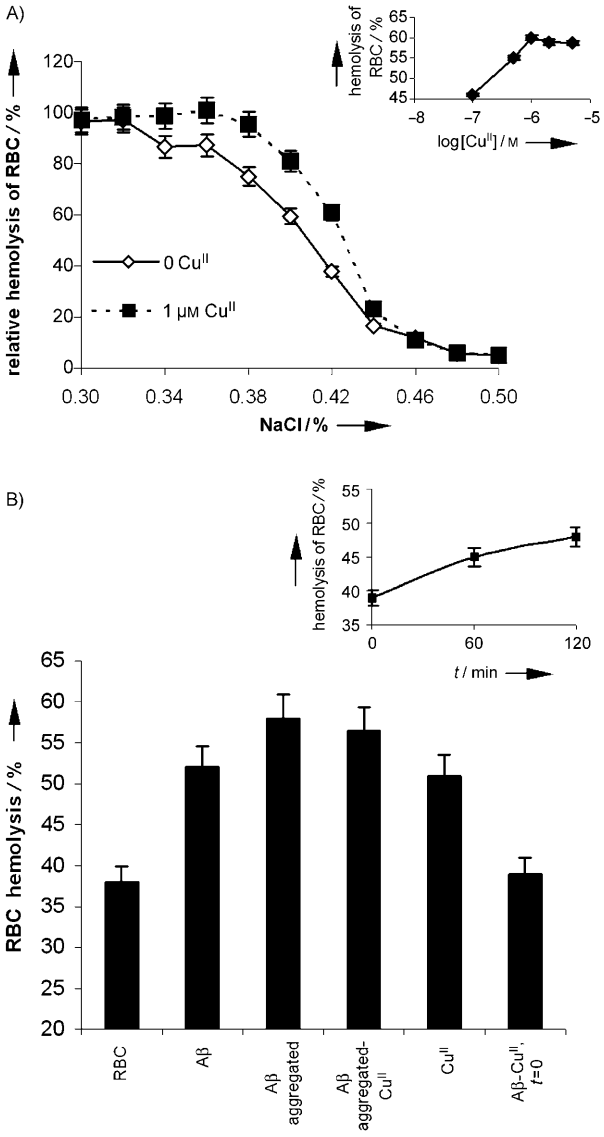

Figure 7. A) Effect of NaCl concentration on the relative haemolysis of RBC. Insert: Influence of Cu^{II} on relative RBC haemolysis at 0.42% NaCl. B) Haemolysis of 30-fold diluted RBC in the presence of 500 nM Aβ, 500 nM Cu^{II} observed at 0.42% NaCl concentration. Insert: Effect of time of complex incubation on the RBC haemolysis at 0.42% NaCl.

Discussion

The main set of findings presented in this study is related to the mechanisms of redox properties of soluble Aβ–copper complexes. We characterise time-dependent changes of the peptide secondary structure induced by Cu^{I} and Cu^{II} binding and correlate these effects with electrochemical properties of the complexes. As previously reported, redox properties of Aβ arise from its ability to bind metals, especially copper.[44] We demonstrated that Aβ is indeed able to bind directly Cu^{I}. Although Aβ–Cu^{I} complexes were isolated from AD brain tissue,[29] previous data suggested that Aβ may reduce Cu^{II} to Cu^{I} and restricted this ability to Aβ42.[25] In our experiments both mono- and divalent metal binding takes place immediately after addition of the monomeric Aβ to PBS; this suggests that Cu^{I} binds to the monomeric, nonaggregated peptide, similarly as the Cu^{II}.[45] The first consequence of metal binding is a change of the peptide hydrophobicity. Slight increase of hydrophobicity due to Cu^{II} binding to Aβ 40, similar to our result, was documented by ANS binding.[46] However, monovalent copper complexation of Aβ in a different way affects peptide hydrophobicity; this implicates a different mode of binding. For the Aβ–Cu^{I} complexes quantum chemical calculations revealed putative distorted-T geometry with histidines and backbone oxygen as possible metal binding ligands.[47] As judged by the differences in the shapes of CD spectra, Aβ–Cu^{I} and Aβ–Cu^{II} complexes probably have different geometries. Although at this stage of investigations the exact determination of Aβ–Cu^{I} geometry it is not possible, the differences between

Aβ–copper complexes of various valences are in accord with general tendency observed for Cu^{I} and Cu^{II} complexes with other ligands that are characterised by a different geometry (usually lower, trigonal or linear for copper of lower valency).[48] Interestingly, low mass bacterial proteins (methanobactins), able to bind both Cu^{I} and Cu^{II}, also generate the CD spectra that differ slightly in the UV region, depending on the valency of copper bound.[49]

Copper binding is capable of inducing conformational changes that affect the aggregation and/or fibrillization processes.[50] Debate concerning the direction of conformational changes induced by Cu^{II} continues, since discordant opinions were presented. Based on the shape of circular dichroism spectrum, it was suggested that copper binding to Aβ40 may induce β-sheet formation,[51] diminish the content of PII-helix,[52] increase both β-sheet and α-helix contents[53] or prevent β-sheet formation.[54] Our CD data analysis suggest that copper binding increase the content of random coil and diminishes amount of β-sheet conformation, proportionally to copper concentrations. A similar tendency was observed by Ricchelli.[46] The discrepancies may result from the fact that copper is coordinated by the nitrogen atoms of histidine residues that may absorb in the far-UV region of the CD spectra. Although this region is most frequently dominated by the peptide bond transitions, even small contributions of side chain transitions to the far-UV spectrum may complicate the conformational analysis. However, molecular dynamic simulations on Aβ42 in solution demonstrated the β-sheet disruption by copper binding to the peptide,[55] consistently with the experimental data. Time dependent studies implicate that conformational changes induced by copper elongate the time in which Aβ–Cu complex is able to attain the same content of β-sheet conformation as for the metal free-peptide. Taking into account that the β-sheet is implicated in the fibrillization process, we hypothesise that this delay may be sufficient to switch the aggregation pathway from fibrillogenic to less structured. Atomic force microscopy (AFM) images obtained by us (Figure S3) and other groups[51] demonstrate striking differences in the morphology of the structures formed by metal-free Aβ in comparison to those generated in the presence of copper and support these suppositions.

Electrochemical properties of Aβ gain a lot of interest. Recently, electrochemical behaviour of Aβ(1–16), Aβ(1–28) and Aβ(1–42) complexes with Cu^{II} (1:1) have been described.[24,56] Redox potentials reported by both groups are close to our observations for Aβ(1–40). However, application of different buffering conditions and different Aβ concentrations resulted in different values of registered reduction potentials of the peptide–Cu^{II} complexes (about 0.25 V (vs. Ag/AgCl) in 50 mM Tris plus 100 mM NaCl[56] and 0.085 V (against Ag/AgCl) in 10 mM phosphate buffer pH 7.4 with 0.1 M Na_2SO_4).[24] The data obtained by us for Aβ(1–40) (0.1 V in 0.2 M KCl and −0.05 V in PBS (both against Ag/AgCl)) are in accord with the observed tendency. Values measured by us are closer to those measured at the similar Aβ concentrations.[24] Additional support for those results come from theoretical modelling study of Rauk group.[47] This study suggests the range of 0.3 to −0.4 V versus SHE (0.08 to −0.62 V vs. Ag/AgCl), as the probable formal potential of Cu^{II}/Cu^{I} couple bound to Aβ. A much higher value of the Aβ redox potential (0.7–0.77 V) was convincingly ascribed to Tyr10 oxidation.[24,57] Moreover, comparison of the potentials measured for Aβ–Cu complexes with literature data concerning reduction potentials of Met35 (1.3 V vs. Ag/AgCl)[58] and Tyr10 (0.77 V vs. Ag/AgCl)[24] support earlier doubts about participation of these residues in the reduction of Aβ–Cu complexes, at least in the conditions of our experiments.[24]

Conflicting results concerning oxidative properties of Aβ have been reported. Several reports documenting oxidative damage of multiple biologically relevant compounds[59] were contrasted to those describing the antioxidative properties of Aβ.[26] In our paper we show that copper complexation by Aβ effectively diminishes the electrochemical signal of the metal (Figures 4, 5, and S1), similarly to the reduction of copper concentration in solution. Additional support for this observation comes from fluorescence (Figure 6). Complexation of substoichiometric to stoichiometric concentrations of copper by Aβ lowered the fluorescence resulting from H_2DCF oxidation by copper. Comparison of the signals generated by the "free" copper and Aβ–Cu complexes suggests antioxidative action of metal binding to the peptide. Thus Aβ could be considered as an antioxidant. Similar results, demonstrating a lower hydroxyl radical formation by Aβ–Cu^{II} complexes than by "unbound" copper ions, were published recently.[56] Another aspect of the Aβ–Cu complex formation is connected with lowering of its reduction potential in comparison with the metal in the solution. As H_2DCF has very low formal reduction potential (about −1.0 V at pH 7.4 against HNE),[39] it can be used to measure redox behaviour of Aβ–copper complexes. The lower potential of the Aβ–Cu^{II} complex means that metal bound by the peptide is more thermodynamically stable than "free" ions in the solution. This signifies that the increased amount of H2DCF has to be oxidized to reduce the same amount of Cu^{II} complexed by the peptide as that of unbound copper. Thus two opposing effects take place simultaneously: lowering of the effective copper concentration that decreases the dye oxidation and a shift of redox potential that increases amount of H_2DCF to be oxidized to reduce complexed copper. The result of these processes is presented in Figure 6A. Assuming that the observed result is a mean of the only two processes, one can conclude that it depends on the copper to the peptide ratio. If metal is present in the complex at substoichiometric to stoichiometric concentrations in proportion to Aβ, complexation exerts prevailing effects. At a moderate excess of Cu^{II} (4–10 times more than the peptide) the impact of complexation and lowering of the redox potential equilibrate. At the higher concentration of Cu^{II}, increased oxidation of H_2DCF is observed; this is consistent with the domination of the lowered redox potential effects. However, one should be aware that the detailed mechanism of the reactions is much more complicated, and the role of copper is not specified yet. In biological systems two-electron oxidation of H_2DCF occurs through two main pathways: reaction catalyzed by peroxidase (or any haem containing protein with peroxidase activity)[39] or directly, by uncatalyzed oxidation (for example, $^{\bullet}OH$ radical, some

metals).[38] As an obligate intermediate, radical $DCFH^{\bullet}$ is formed and then reacts with oxygen, resulting in DCF formation. This general mechanism is probably preserved in reactions involving copper, as deaeration of the solutions and inert atmosphere inhibit the oxidation process. However, as described by Wrona and Wardman,[39] the radical $DCFH^{\bullet}$ has several prototropic and resonance forms and detailed mechanism of copper action during oxidation to DCF according to our best knowledge has not been studied yet. Although our previous paper suggested superoxide- and singlet oxygen-mediated oxidation of H_2DCF under redox-active-metal enhanced conditions,[60] reported self-induced $O_2^{\bullet-}/H_2O_2$ production during the dye oxidation[61] force us to be cautious in the extrapolating the data to more physiological conditions. Thus, on the basis of our experiments, it is very hard to hypothesise on the role of copper in the process of H_2DCF oxidation and/or kind of reactive oxygen species formed.

An aggregational studies that investigate the effects of Aβ40 complexation by substoichiometric to excessive concentrations of copper show fast, nonfibrillar aggregation of the latter.[62] In our experiments, an increase in copper concentration proportional to Aβ resulted in an increase of the dye oxidation, more pronounced than that caused by copper alone (Figure 6). In addition, voltammetric study revealed appearance of a second peak of reduction, shifted towards more negative values (Figure 5). This may suggest that complexes containing excess of copper may possess quite significant redox activity, which may be present even in the aggregated state.

Aβ is present in blood at nanomolar levels.[63] Fibrillar aggregates of Aβ are deposited in blood vessels.[64] Alteration of RBC membranes in AD donors was observed as determined by the amyloid induced membrane lipid peroxidation and lysis.[65] In contrast to Aβ25–35, interaction with RBC membranes of longer Aβ40 does not result in membrane lysis; this suggests that other mechanisms could be involved. The interaction of fibrillar Aβ40 with RBCs increased the mean cell volume, caused cells to be more spherical and induced oxidative degradation of haem.[43]

Cytotoxic action of Cu^{II}, as determined by its ability to enhance haemolysis under hypotonic conditions, was enhanced in the presence of the copper–amyloid complex; this suggests that membrane damage could result from the oxidative property of the complex. The ability of antioxidants to protect neurones[8] and blood cells[57] against β-amyloid toxicity supports the redox character of the observed phenomenon. Under our experimental conditions complexation of copper by Aβ diminish the RBC haemolysis, in a similar way as binding of copper to albumin and ceruloplasmin decreased rates of the RBC haemolysis.[66] However, prolonged incubation with the cells causes gradual haemolysis; this is consistent with fluorescence and voltammetric data implicating that Aβ–Cu complexes still possess oxidative properties. In contrast, fibrillar Aβ did not demonstrate this protective function, and induced haemolysis similar to that of unbound copper ions.

Our results point to a protective role of copper complexation by Aβ that can probably diminish oxidative stress, by lowering the effective free copper in brain fluids. β-Amyloid folding, although affected by copper, is probably the additional mechanism that allows diminished accessibility of the metal for redox active agents. However, along with the progress of the disease, the low redox properties of Aβ-complexes may become the more detrimental to surrounding tissue, primarily due to their increased concentration.

Although further studies are required to verify the physiological relevance of the reported phenomena in vivo, they imply potential pharmacological strategies that are based on inhibition of cellular damage resulting from copper-mediated oxidative stress.

Conclusions

This report describes the mechanism related to the oxidative properties of Aβ40 in the presence of copper. We show that Aβ40 is able to form complexes of different hydrophobicities and conformations both with mono- and divalent copper. Complexation of the metal by Aβ results in diminished concentration of electrochemically active ions. In this respect, Aβ plays an antioxidative role. However, the copper binding to Aβ is not tantamount to the lack of electrochemical activity. Redox properties of Aβ–Cu complexes still exist, and formal reduction potential of Aβ–Cu complexes is shifted towards more negative values than that of the free ion. Moreover, the conformational rearrangements, especially well visible at copper excess, lead to an increase of the less labile species characterised by the lower redox potential with a concomitant decrease of those reduced at the higher potential. Extrapolating, this property of Aβ complexes may be responsible for the oxidative modification of a wider spectrum of biologically active compounds than one could expect from the copper ions. The presented results are therefore consistent with oxidative damage observed in the vicinity of senile plaques in AD brains.

Experimental Section

Sample preparation: β-Amyloid (1–40) peptide was purchased from AnaSpec (San Jose, CA, USA) and Sigma–Aldrich. The peptide was dissolved in dimethyl sulfoxide (DMSO) to assure monomericity or deionised water (for CD measurements), aliquoted and stored at −20 °C. 4,4′-Dianilino-1,1′-binaphthyl-5,5′-disulfonic acid (bisANS) was purchased from Sigma–Aldrich. Phen Green™ (PG) and 2′,7′-dichlorodihydrofluorescein diacetate (H_2DCF-DA) were sold by Molecular Probes. Ficoll separating solution (density 1.077 g mL^{-1}) was a product of Biochrom AG (Berlin, Germany). All other chemicals were from Sigma–Aldrich.

$CuCl_2$ and CuCl were dissolved in deionised and chelex-100-treated water and used fresh on the same day. Water used for preparation of CuCl solutions was additionally deaerated and saturated with nitrogen. CuCl solutions were kept under nitrogen. Reducing agents like ascorbate or hydroxylamine were not used, to avoid possible interference with the peptide and/or other reactants. As Cu^{I}–water solutions may be unstable due to disproportionation to Cu^{0} and Cu^{II}, we checked Cu^{I} content using a bathocuproine-based fluorescence quenching method. Cu^{I} concentration changes of deaerated solutions during 1 h did not exceed 2% of the initial value, which was comparable to the experimental error. However, for the long

lasting experiments, we have to mention the possibility of partial disproportionation of Cu^{I}.

Fluorescence measurements: Fluorescence measurements were performed using a SPEX Fluorolog 3 fluorometer or Perkin–Elmer LS 5B spectrometer. Background fluorescence (buffer, reporting dye, metal) was subtracted from each measurement.

Copper binding: Quenching of PG, a fluorescent dye sensitive to copper ions, was used to determine Aβ–Cu^{II} and/or Aβ–Cu^{I} complex formation ($\lambda_{ex}=488$ nm, $\lambda_{em}=517$ nm).[30] Copper (1×10^{-7} M), peptide (10^{-7} M) and Phen Green™ (2×10^{-7} M) in 3-(*N*-morpholine)-sulfonic acid (5 mM, MOPS) buffer were applied. PG relative fluorescence quenching was defined as $F_{PG}-F_{PG(Cu)}$ or $F_{PG}-F_{PG(A\beta-Cu)}$.

Copper(I) stability: The quenching of 10–6 M bathocuproine disulphonate solutions in PBS ($\lambda_{ex}=580$ nm, $\lambda_{em}=770$ nm) was used to measure Cu^{I} content, according to the procedure described by Rapisarda and coauthors.[41]

Hydrophobicity assay: Exposure of Aβ hydrophobic surface was measured as an increase of bisANS fluorescence resulting from binding to the Aβ–copper complex.[66] A ratio of Aβ to metal ions was 1:5 (mol/mol). 2×10^{-5} M of the peptide and 2×10^{-4} M of bisANS concentrations were applied. Aβ–Cu complexes were incubated for indicated periods of time, then mixed with bisANS, and measured within 5 min ($\lambda_{ex}=395$ nm, $\lambda_{em}=460$–560 nm).

Fluorescence redox determination: Redox activity of Aβ in the presence of metal ions was monitored by increase of H_2DCF fluorescence due to its oxidation to DCF ($\lambda_{ex}=504$ nm, $\lambda_{ex}=525$ nm). H_2DCF was obtained by hydrolysis of its diacetate ester as described previously.[60] H_2DCF concentration was 10^{-7} M, redox reaction time = 1 h. Solutions were not deaerated.

Circular dichroism spectral measurements: CD spectra were recorded on a Aviv 206 CD spectrometer at room temperature. The spectral range was 190–250 nm with a resolution of 1 nm and bandwidth 1 nm. Averaging time and response time were 1 s. The optical path length of cell was 0.1 cm. Ratio of Aβ to metal ions was 1:2 (mol/mol). Concentration of Aβ was 10^{-5} M. The CD measurements were carried out in vacuum-deaerated phosphate buffer (50 mM, pH 7.2) with KF (0.15 M) under nitrogen atmosphere. The influence of copper on Aβ conformation was measured immediately after mixing and after 2 h of incubation. The content of secondary structural elements was assessed by CD neural Network program (CDNN).[68]

Voltammetry: Cyclic voltammetry (CV) and differential pulse voltammetry (DPV) experiments were performed using the Autolab potentiostat (ECO Chemie, Utrecht, the Netherlands, equipped with GPES software) in a three electrode arrangement with a Ag/AgCl electrode as the reference, platinum foil as the counter and glassy carbon electrode (GCE, BAS, 3 mm diameter) as the working electrode. KCl (0.2 M) in highly purified water (18.6 MΩ, Milli-Q system (Millipore, Milford, CT, USA)) was used as the supporting electrolyte solution (pH 6,9). In CV experiments sweep rate was 0.05 V s^{-1}. In DPV pulse potential applied was 0.03 V, time of pulse duration 0.01 s. Argon was used to deaerate the solution and argon blanket was maintained over the solution during the experiments. Concentrations of $CuCl_2$ solutions lower than 10^{-4} M were used to avoid slow precipitation of copper salt. All experiments were carried out at room temperature.

AFM Imaging: AFM imaging was performed on a Digital Instrument CP-II (Veeco Instrument Inc., Santa Barbara, CA, USA) equipped with 100 μm scanner. Digital Instrument CP-II was situated on vibration isolation table (Technical Manufacturing Corporation, Peabody, MA, USA). All images were taken in the noncontact AFM imaging mode, in air, at room temperature (22–25 °C). Silicon OTESPA probes (Veeco Probes, Camarillo, CA, USA) with a nominal spring constant of 42 N m^{-1} and resonance frequency of 300 kHz were used. The set point and gain was adjusted in order to obtain stable imaging conditions and minimize noises. Typical scan rate was 1 Hz. The scan size was 5×5 μm. The images were sampled at resolution of 256×256 points. To obtain representative images and data, three or more different surface fragments of each sample were scanned. ProScan Image Processing version 2.1 was used to flatten images to remove background slope and small artifacts. This program was also used to generate 2D images and height profiles. Veeco DI SPMLab NT program Ver.6.0.2 was used to generate 3D images. Sample preparation: Aβ (50×10^{-6} M) was incubated for 1 or 48 h in chelex-100 treated PBS or in the above buffer supplemented with Cu^{II} (peptide to metal proportion 1:1, mol/mol). The mixture (5×10^{-6} L) was transferred on freshly cleaved mica, incubated for 5 min and washed with deionised water (200×10^{-6} L). After removing the excess of water by spongy paper, the sample was left to dry for at least 1 h, and scanned.

RBCs as a model of Aβ–Cu^{II} complex toxicity: RBCs were extracted from heparinised blood obtained by venipuncture from healthy volunteers from 25 to 30 years old, after having obtained written consent, by standard Ficoll procedure.[69] To determine the stability of RBC membranes in the presence of Cu^{II} ions and Aβ we assayed the level of haemoglobin release from RBC induced by hypotonic lysis (at 0.42% NaCl) using absorption measurements. Absorption measurements (450 nm) were performed using the microplate reader Model 550, BioRad.

Acknowledgements

This work was supported by Center of Excellence "MIND" and the Polish Committee for Scientific Research as grant 3P05F 00524 in 2003–2007.The research was partially supported by the European Union through grant Innovative Economy (POIG.01.01.02-00-008/08).

Keywords: copper · electrochemistry · fluorescence spectroscopy · peptides · protein folding

[1] C. A. McLean , R. A. Cherny, F. W. Fraser, S. J. Fuller, M. J. Smith, K. Beyreuther, A. I. Bush, C. L. Masters, *Ann. Neurol.* **1999**, *46*, 860–866.
[2] D. R. Canning, R. J. McKeon, D. A. DeWitt, G. Perry, J. R. Wujek, R. C. Frederickson, J. Silver, *Exp. Neurol.* **1993**, *124*, 289–298.
[3] A. Nunomura, R. J. Castellani, X. Zhu, P. I. Moreira, G. Perry, M. A. Smith, *J. Neuropathol. Exp. Neurol.* **2006**, *65*, 631–641.
[4] C. D. Smith, J. M Carney, P. E. Starke-Reed, C. N. Oliver, E. R. Stadtman, R. A. Floyd, W. R. Markesbery, *Proc. Natl. Acad. Sci. USA* **1991**, *88*, 10540–10543.
[5] K. Hensley, J. M. Carney, M. P. Mattson, M. Aksenova, M. Harris, J. F. Wu, R. A. Floyd, D. A. Butterfield, *Proc. Natl. Acad. Sci. USA* **1994**, *91*, 3270–3274.
[6] E. R. Stadtman, R. L. Levine, *Neurobiol. Aging* **1999**, *20*, 331–333; *Neurobiol. Aging* **1999**, *20*, 339–342.
[7] R. J. Mark, M. A. Lovell, W. R. Markesbery, K. Uchida, M. P. Mattson, *J. Neurochem.* **1997**, *68*, 255–264.
[8] C. Behl, J. B. Davis, R. Lesley, D. Schubert, *Cell* **1994**, *77*, 817–827.
[9] M. A. Lovell, J. D. Robertson, W. J. Teesdale, J. L. Campbell, W. R. Markesbery, *J. Neurol. Sci.* **1998**, *158*, 47–52.
[10] X. Huang, M. P. Cuajungco, C. S. Atwood, M. A. Hartshorn, J. D. Tyndall, G. R. Hanson, K. C. Stokes, M. Leopold, G. Multhaup, L. E. Goldstein, R. C.

Scarpa, A. J. Saunders, J. Lim, R. D. Moir, C. Glabe, E. F. Bowden, C. L. Masters, D. P. Fairlie, R. E. Tanzi, A. I. Bush, *J. Biol. Chem.* **1999**, *274*, 37111–37116.
[11] G. F. da Silva, W. M. Tay, L. J. Ming, *J. Biol. Chem.* **2005**, *280*, 16601–16609.
[12] P. Zatta, G. Tognon, P. Carampin, *J. Pineal Res.* **2003**, *35*, 98–103.
[13] C. Schöneich, T. D. Williams, *Chem. Res. Toxicol.* **2002**, *15*, 717–722.
[14] T. Miura, K. Suzuki, N. Kohata, H. Takeuchi, *Biochemistry* **2000**, *39*, 7024–7031.
[15] C. S. Atwood, R. C. Scarpa , X. Huang , R. D. Moir , W. D. Jones , D. P. Fairlie, R. E. Tanzi, A. I. Bush, *J. Neurochem.* **2000**, *75*, 1219–1233.
[16] C. D. Syme, R. C. Nadal, S. E. Rigby, J. H. Viles, *J. Biol. Chem.* **2004**, *279*, 18169–18177.
[17] O. N. Antzutkin, *Magn. Reson. Chem.* **2004**, *42*, 231–246.
[18] G. A. Rickard, R. Gomez-Balderas, P. Brunelle, D. F. Raffa, A. Rauk, *J. Phys. Chem. A* **2005**, *109*, 8361–8370.
[19] J. W. Karr, H. Akintoye, L. J. Kaupp, V. A. Szalai, *Biochemistry* **2005**, *44*, 5478–5487.
[20] W. Garzon-Rodriguez, A. K. Yatsimirsky, C. G. Glabe, *Bioorg. Med. Chem. Lett.* **1999**, *9*, 2243–2248.
[21] L. Hou, M. G. Zagorski, *J. Am. Chem. Soc.* **2006**, *128*, 9260–9261.
[22] K. J. Barnham, F. Haeffner, G. D. Ciccotosto, C. C. Curtain, D. Tew, C. Mavros, K. Beyreuther, D. Carrington, C. L. Masters, R. A. Cherny, R. Cappai, A. I. Bush, *FASEB J.* **2004**, *18*, 1427–1429.
[23] C. Schöneich, D. Pogocki, G. L. Hug, K. Bobrowski, *J. Am. Chem. Soc.* **2003**, *125*, 13700–13713.
[24] D. Jiang, L. Men, J. Wang, Y. Zhang, S. Chickenyen, Y. Wang, F. Zhou, *Biochemistry* **2007**, *46*, 9270–9282.
[25] S. Varadarajan, J. Kanski, M. Aksenova, C. Lauderback, D. A. Butterfield, *J. Am. Chem. Soc.* **2001**, *123*, 5625–5631.
[26] A. Kontush, *Free Radical Biol. Med.* **2001**, *31*, 1120–1131.
[27] J. Lee, M. M. Peña, Y. Nose, D. J. Thiele, *J. Biol. Chem.* **2002**, *277*, 4380–4387.
[28] H. Gunshin, B. Mackenzie, U. V. Berger, Y. Gunshin, M. F. Romero, W. F. Boron, S. Nussberger, J. L. Gollan, M. A. Hediger, *Nature* **1997**, *388*, 482–488.
[29] R. A. Cherny, J. T. Legg, C. A. McLean, D. P. Fairlie, X. Huang, C. S. Atwood, K. Beyreuther, R. E. Tanzi, C. L. Masters, A. I. Bush, *J. Biol. Chem.* **1999**, *274*, 23223–23228.
[30] R. P. Haugland, *Handbook of Fluorescent Probes and Research Chemicals*, 6th ed., Molecular Probes Inc, **1996**, pp. 533–540.
[31] M. Brzyska, K. Trzesniewska, T. Gers, D. Elbaum, *FEBS J.* **2006**, *273*, 5598–5611.
[32] Y. R. Chen, C. G. Glabe, *J. Biol. Chem.* **2006**, *281*, 24414–24422.
[33] J. J. Kremer, D. J. Sklansky, R. M. Murphy, *Biochemistry* **2001**, *40*, 8563–8571.
[34] a) N. Sreerama, R .W. Woody in *Circular Dichroism: Principles and Applications* (Eds.: N. Berova, K. Nakanishi, R. W. Woody), Wiley-VCH, Weinheim, **2000**, pp. 601–620; b) A. Koslowski, N. Sreerama, R. W. Woody in *Circular Dichroism: Principles and Applications* (Eds.: N. Berova, K. Nakanishi, R. W. Woody), Wiley-VCH, Weinheim, **2000**, p. 76.
[35] R. G. Compton, C. E. Banks, *Understanding Voltammetry*, World Scientific, New Jersey, **2007**, pp. 107–152 and 342–343.
[36] K. Słowinski, *Ph.D. Thesis*, Warsaw University (Poland), **1997**.
[37] P. D. Beer, P. A. Gale, G. Z. Chen, *Coord. Chem. Rev.* **1999**, 185–186, 3–36.
[38] K. D. Sugden, K. M. Rigby, B. D. Martin, *Toxicol. In Vitro* **2004**, *18*, 741–748.
[39] M. Wrona, P. Wardman, *Free Radical Biol. Med.* **2006**, *41*, 657–667.
[40] H. Laggner, M. Hermann, B. M. Gmeiner, S. Kapiotis, *Anal. Bioanal. Chem.* **2006**, *385*, 959–961.
[41] V. A. Rapisarda, S. I. Volentini, R. N. Farias, E. M. Massa, *Anal. Biochem.* **2002**, *307*, 105–109.
[42] R. A. Løvstad, *Int. J. Biochem.* **1982**, *14*, 585–589.
[43] R. Jayakumar, J. W. Kusiak, F. J. Chrest, A. A. Demehin, J. Murali, R. P. Wersto, E. Nagababu, L. Ravi, J. M. Rifkind, *Biochim. Biophys. Acta Gen. Subj.* **2003**, *1622*, 20–28.
[44] S. I. Dikalov, M. P. Vitek, K. R. Maples, R. P. Mason, *J. Biol. Chem.* **1999**, *274*, 9392–9399.
[45] C. Talmard, L. Guilloreau, Y. Coppel, H. Mazarguil, P. Faller, *ChemBioChem* **2007**, *8*, 163–165.
[46] F. Ricchelli, D. Drago, B. Filippi, G. Tognon, P. Zatta, *Cell. Mol. Life Sci.* **2005**, *62*, 1724–1733.
[47] D. F. Raffa, G. A. Rickard, A. Rauk, *J. Biol. Inorg. Chem.* **2007**, *12*, 147–164.
[48] M. C. Machczynski, H. B. Gray, J. H. Richards, *J. Inorg. Biochem.* **2002**, *88*, 375–380.
[49] D. W. Choi, C. J. Zea, Y. S. Do, J. D. Semrau, W. E. Antholine, M. S. Hargrove, N. L. Pohl, E. S. Boyd, G. G. Geesey, S. C. Hartsel, P. H. Shafe, M. T. McEllistrem, C. J. Kisting, D. Campbell, V. Rao, A. M. de La Mora, A. A. Dispirito, *Biochemistry* **2006**, *45*, 1442–1453.
[50] Y. Yoshiike, K. Tanemura, O. Murayama, T. Akagi, M. Murayama, S. Sato, X. Sun, N. Tanaka, A. Takashima, *J. Biol. Chem.* **2001**, *276*, 32293–32299.
[51] A. K. Tickler, D. G. Smith, G. D. Ciccotosto, D. J. Tew, C. C. Curtain, D. Carrington, C. L. Masters, A. I. Bush, R. A. Cherny, R. Cappai, J. D. Wade, K. J. Barnham, *J. Biol. Chem.* **2005**, *280*, 13355–13363.
[52] J. Danielsson, R. Pierattelli, L. Banci, A. Gräslund, *FEBS J.* **2007**, *274*, 46–59.
[53] X. L. Dai, Y. X. Sun, Z. F. Jiang, *Acta Biochim. Biophys. Sin.* **2006**, *38*, 765–772.
[54] B. Raman, T. Ban, K. Yamaguchi, M. Sakai, T. Kawai, H. Naiki, Y. Goto, *J. Biol. Chem.* **2005**, *280*, 16157–16162.
[55] D. F. Raffa, A. Rauk, *J. Phys. Chem. A* **2007**, *111*, 3789–3799.
[56] L. Guilloreau, S. Combalbert, A. Sournia-Saquet, H. Mazarguil, P. Faller, *ChemBioChem* **2007**, *8*, 1317–1325.
[57] M. Vestergaard, K. Kerman, M. Saito, N. Nagatani, Y. Takamura, E. Tamiya, *J. Am. Chem. Soc.* **2005**, *127*, 11892–11893.
[58] Sanaullah, G. S. Wilson, R. S. Glass, *J. Inorg. Biochem.* **1994**, *55*, 87–99.
[59] C. Opazo, X. Huang, R. A. Cherny, R. D. Moir, A. E. Roher, A. R. White, R. Cappai, C. L. Masters, R. E. Tanzi, N. C. Inestrosa, A. I. Bush, *J. Biol. Chem.* **2002**, *277*, 40302–40308.
[60] M. Brzyska, A. Bacia, D. Elbaum, *Eur. J. Biochem.* **2001**, *268*, 3443–3454.
[61] M. G. Bonini, C. Rota, A. Tomasi, R. P. Mason, *Free Radical Biol. Med.* **2006**, *40*, 968–975.
[62] D. P. Smith, G. D. Ciccotosto, D. J. Tew, M. T. Fodero-Tavoletti, T. Johanssen, C. L. Masters, K. J. Barnham, R. Cappai, *Biochemistry* **2007**, *46*, 2881–2891.
[63] P. Seubert, C. Vigo-Pelfrey, F. Esch, M. Lee, H. Dovey, D. Davis, S. Sinha, M. Schlossmacher, J. Whaley, C. Swindlehurst, *Nature* **1992**, *359*, 325–327.
[64] R. N. Kalaria, D. R. Premkumar, A. B. Pax , D. L. Cohen, I. Lieberburg, *Brain Res. Mol. Brain. Res.* **1996**, *35*, 58–68.
[65] M. P. Mattson, J. G. Begley, R. J. Mark, K. Furukawa, *Brain Res.* **1997**, *771*, 147–153.
[66] J. M. Caffrey, Jr., H. A. Smith, J. C. Schmitz, A. Merchant, E. Frieden, *Biol. Trace Elem. Res.* **1990**, *25*, 11–19.
[67] H. LeVine, 3rd, *Arch. Biochem. Biophys.* **2002**, *404*, 106–115.
[68] G. Böhm, R. Muhr, R. Jaenicke, *Protein Eng.* **1992**, *5*, 191–195.
[69] A. Ferrante, Y. H. Thong, *J. Immunol. Methods* **1982**, *48*, 81–85.

Received: November 7, 2008
Published online on March 4, 2009

